Nano Express

PAPER • OPEN ACCESS

Wet etching of gold on graphene for high-quality resist-free graphene surfaces

To cite this article: J Kunc *et al* 2023 *Nano Ex.* **4** 035006

View the article online for updates and enhancements.

You may also like

- Comparison of three digestion methods for determination of selenium in green tea samples using fluorescence spectrometry
S R Kamali, C H Tsai and C N Chen
- Evaluation of Titanium Carbide Thin Film Coatings on Surface Microstructure Controlled WC-Co
Chihiro Tanaka, Takeyasu Saito, Naoki Okamoto et al.
- Platinum Recovery from Spent CCR Platforming Catalyst with Oxalic Acid and Aqua Regia Leaching
Yuliusman, L P D I Prawira, A R Nafisah et al.

This content was downloaded from IP address 195.113.35.185 on 13/09/2023 at 15:42

NANO EXPRESS

OPEN ACCESS

RECEIVED
19 July 2023

REVISED
5 August 2023

ACCEPTED FOR PUBLICATION
11 August 2023

PUBLISHED
29 August 2023

Original content from this work may be used under the terms of the Creative Commons Attribution 4.0 licence.

Any further distribution of this work must maintain attribution to the author(s) and the title of the work, journal citation and DOI.

PAPER

Wet etching of gold on graphene for high-quality resist-free graphene surfaces

J Kunc[1], M Shestopalov[1], J Jo[2] and K Park[2]

[1] Charles University, Faculty of Mathematics and Physics, Institute of Physics, Ke Karlovu 5, Prague 2, CZ-121 16, Czech Republic
[2] Ulsan National Institute of Science and Technology, Department of Physics, 50 UNIST-Gil Eonyang-Eup Ulju-Gun, 44919 Ulsan, Republic of Korea

E-mail: jan.kunc@matfyz.cuni.cz

Keywords: wet etching of gold on graphene, over-exposure, hard-bake, post-development bake, aqua regia wet etch, bubble formation and elimination, resist adhesion enhancement

Abstract

Wet etching of gold on graphene is challenging due to the weak adhesion of the resist mask to graphene. We report an operating procedure for alkali ion-free wet etching of gold on graphene using a mixture of hydrochloric and nitric acids (aqua regia) with a high lateral resolution down to 100 nm. We investigate the role of positive and negative resists, electron beam lithography (EBL) dose, hard-bake, oxygen etching, aging, and sensitivity to the etch parameters, such as the freshness of dilute aqua regia, etch time, and the order of etched samples. The negative-tone resist provides the best results. The over-dosed EBL exposure can enhance the resist adhesion, as hard-bake below the glass-transition temperature and well-defined wet etch of the resist-residua-free gold surface. We also present a cleaning procedure to avoid bubble formation after the hard bake. Our results demonstrate that wet etching of gold on graphene using aqua regia is a viable method for achieving high-quality resist-free graphene surfaces. This method has potential applications in graphene nanoelectronics and nanophotonics, where high-quality graphene surfaces are essential for device performance.

1. Introduction

Microfabrication uses polymer resists to imprint the desired structures into the material of interest. The two-dimensional graphene crystals present a significant challenge in such polymer-based processing. The spin-coated polymers leave residual trances on the graphene surface, which are hard to remove entirely. The resist residua deteriorate graphene mobility [1–3] and modify doping in graphene [1, 4] via formation of polymeric residue/hydrogen-functionalization [5]. Since the residual resist can be up to 1 to 2nm thick [6], it is also prohibitive to use graphene in surface-sensitive plasmonic applications [7] or to fabricate reliable tunneling barriers with other graphene or metal electrodes [8]. The tunneling is a fast transport mechanism that could be used for high-speed graphene rectifiers, as demonstrated for metal-insulator-metal diodes [9], with the advantage of atomic thickness, smaller capacitance, and faster response times. However, the graphene-oxide-metal interface must be sharp on the nanometer length scale to fully exploit its potential for electro-optical applications [10]. Standard methods to remove the residual resist layer are the thermal annealing [1, 5, 11], plasma treatments [12, 13], wet etching [14], mechanical cleaning using an atomic force microscopy tip [2, 3], or electrical current [15]. Unfortunately, the most common thermal annealing leads to sp^2 to sp^3 conversion with increasing time and temperature [4], and deteriorating graphene quality at annealing temperature above 650 °C [16]. The thermal annealing also increases the interaction of graphene with the substrate, thus lowering the graphene mobility [11]. This mobility reduction occurs because the annealing induces strain by pinning graphene more strongly to the substrate [5]. Also, the contamination only rarely vanishes entirely [2, 12, 15]. Although some techniques are promising [14], the number of research papers on the topic, including review papers [13], demonstrates that cleaning the PMMA residua from graphene is cumbersome. Also, the graphene cleaning procedure might vary based on the substrate and the type of graphene. The cleaning procedures

© 2023 The Author(s). Published by IOP Publishing Ltd

reported on substrates such as SiO_2 [17] or $SrTiO_3$ [18] might differ from the graphene cleaning procedures on, e.g., SiC. Besides the substrate, the CVD graphene has edges exposed to the external environment making the CVD graphene highly reactive at the edges. On the other hand, epitaxial graphene on SiC is covalently bonded to the SiC substrate [19], making the epitaxial graphene edges chemically inert. Thus, we exploit a different approach suitable for graphene grown epitaxially on SiC. The technique relies on a protection layer deposited on graphene before the spin-coating, as discussed by Lin *et al* [4] and realized by Yang *et al* [20]. The gold protection layer is deposited in the first processing step and removed in the last step. Yang *et al* demonstrated the benefits of the gold reaching low carrier density in epitaxial graphene on SiC and high carrier mobility. The low carrier density and high mobility are beneficial for the resistance standard applications [21, 22], where the combination of the Fermi level pinning and low doping is essential [23]. The remaining challenge is to remove gold using the resist mask. The gold etching should not modify graphene; it should provide high lateral resolution and low under-etching and not deteriorate oxide-insulating properties in the following microfabrication steps. A common and relatively non-aggressive wet etchant is a KI and I_2 mixture [24]. However, the alkali ions, the residual potassium, quickly diffuse in oxides, thus degrading their electrical insulation [25, 26]. Instead, the hydrochloric and nitric acid mixture, the aqua regia, must be used to keep the sample's surface clean of residual alkali ions and effectively etch gold. The pure aqua regia is a strong etchant, and the problems with the resist adhesion to the substrate can cause severe lateral etching of gold, resist etching, peeling, or swelling. These issues can be resolved by diluting the aqua regia with deionized (DI) water [20]. Although the basic principles of the wet etching of gold by diluted aqua regia (DAR) are known [20], the research on gold wet etching is still ongoing [27, 28]. And in contrast to many other metals, wet etching remains an essential process in microfabrication [29] because of its low cost, high throughput, and easily controllable etch rate [30].

In this work, we report a detailed step-by-step technology to achieve a high-resolution wet etching of gold on epitaxial graphene on SiC without large lateral etching and under-etching. The resist adhesion to the substrate is critical in reducing lateral etching. We propose a combination of adhesion-enhancing processes that result in the final good lateral etch resolution. The resist selection is the first step. We demonstrate better mask properties of the negative novolak resist than the positive PMMA. The advantage of the negative resist is that the increased dose can enhance its adhesion to the substrate during the electron beam lithography (EBL). In both cases, positive and negative resist adhesion can be enhanced by the post-development hard-bake [31, 32]. We also propose the pre-etching residual resist ashing and demonstrate the role of precise timing in the DAR etching and freshness of the DAR solution. The strength of the DAR etchant quickly deteriorates; hence, the etching properties differ also with the number of etched samples. We report under-etching on the order of 100's nm, which is competitive to the state-of-the-art technology with documented 1–3 μm under-etch [27] using a KI and I_2 mixture. In our DAR etching, we avoid contamination by alkali ions and yet report the improved etch lateral resolution.

2. Methods

We grew epitaxial graphene by thermal decomposition of SiC. We purchased the SiC wafers at II-VI, Inc. and Wolfspeed, Inc. The wafers were diced into 5x5 mm samples and cleaned in acetone, methanol, isopropanol, and distilled water (AMIW cleaning). The SiC samples were loaded in a graphite crucible. We use a hot-wall RF furnace to heat the graphite crucible in an argon atmosphere to 1650 °C for 5 mins, as we demonstrated in detail, including *in situ* analysis of the residual gases, in our previous work [33].

The following sample treatment is a part of the wet etching procedure described throughout this paper. The general procedure involves post-growth cleaning and gold evaporation to protect graphene from contact with the spin-coated resist, resist spin-coating, and wet etching. The gold protection layer was 30 nm thick, and we compared positive (AR-P 679.04, PMMA) and negative resist (AR-N 7520.17new, novolak based) purchased at Allresist GmbH. The DAR was used throughout this work. We use a mixture of 1 part of HNO_3 (5 ml, 69%), 4 parts of HCl (20 ml, 37%), and 4 parts (20 ml) of deionized (DI) water. We always etch two samples in one etching procedure. If more samples are needed to be etched, we prepare a new batch of DAR. The etching was performed at room temperature and was always done using a fresh DAR within 1-2 minutes after preparing 50 ml of DAR when the solution was still warm after mixing.

3. Results

3.1. Under-etched resist and bubble formation

Figure 1 compares the common issues with the (a), (d), (e) positive and (b), (c), (f), (g) negative resist used as a mask for wet etching of gold in DAR. Both show poor adhesion to the gold layer. The poor adhesion leads to severe under-etching on the order of 30 μm in the case of PMMA, figure 1(a), and floating of small structures

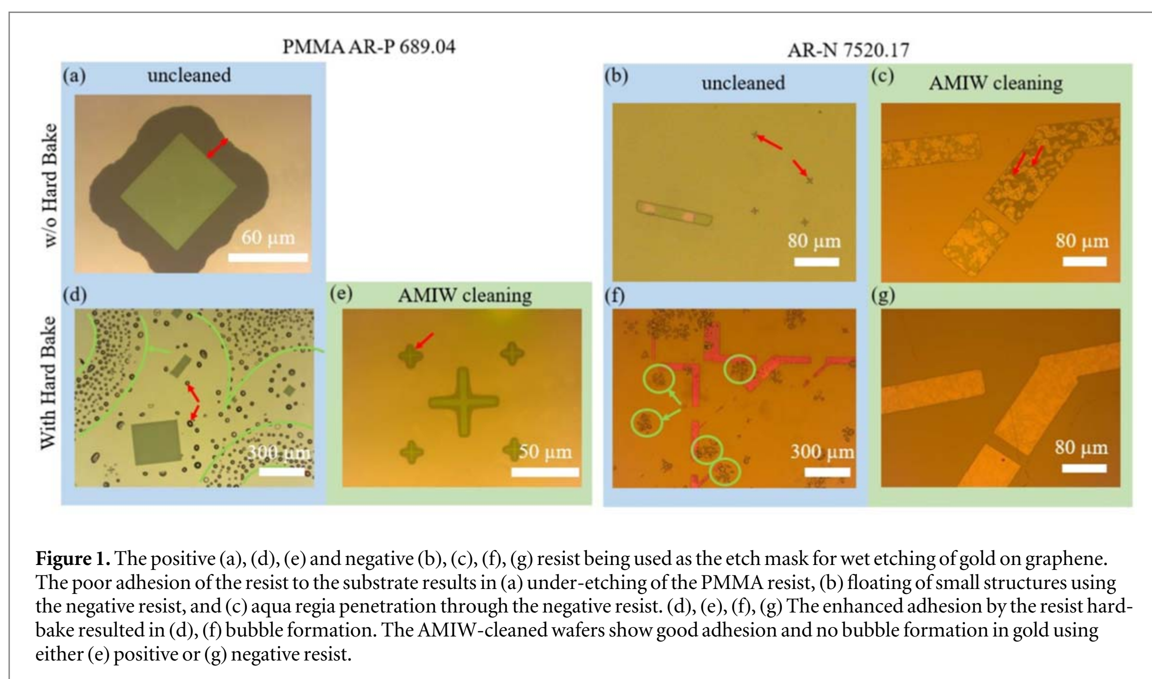

Figure 1. The positive (a), (d), (e) and negative (b), (c), (f), (g) resist being used as the etch mask for wet etching of gold on graphene. The poor adhesion of the resist to the substrate results in (a) under-etching of the PMMA resist, (b) floating of small structures using the negative resist, and (c) aqua regia penetration through the negative resist. (d), (e), (f), (g) The enhanced adhesion by the resist hard-bake resulted in (d), (f) bubble formation. The AMIW-cleaned wafers show good adhesion and no bubble formation in gold using either (e) positive or (g) negative resist.

defined by the negative resist, figure 1(b). We hard-baked the developed resists before the wet etching to enhance the resist adhesion. The hard bake reduced the PMMA/novolak under etching to the order of 2 μm/100 nm. However, the thermal treatment and different thermal expansion coefficients of the SiC substrate, gold layer, and resist led to the bubble formation. The bubbles seem to avoid patterned regions in PMMA, figure 1(d), depicted by green regions. There are also sparsely distributed bubbles without any correlation to the developed patterns in the resist, two red arrows in figure 1(d). The contamination most likely causes sparse, randomly distributed bubbles. We ascribe the large domains of gathered bubbles, green regions in figure 1(d), to the mechanical strain between the SiC substrate and gold layer. The missing positive resist in the exposed pattern is a source of the spatially uneven mechanical strain spatial distribution. The case of negative resist is different. Since there are no large domains of negative resist, the mechanical strain is relaxed and only the contamination causes the bubble formation, figure 1(f). The contamination-related bubbles form small islands, green circles in figure 1(f), indicating that the contamination has been present on the sample's surface before the gold deposition, and it does not come from a metal source in the electron beam evaporator. We expect no bubble bunching and homogeneous bubble formation in the latter case. We avoided bubble formation by cleaning the epitaxial graphene on SiC before the gold evaporation. The cleaning involved 5 min in acetone, 5 min in methanol, 5 min in isopropanol (IPA), 10 min in DI water (AMIW cleaning). The hot plate bake at 250 °C followed the wet cleaning for 900 s to remove residual water from the graphene surface. We note that the bubbles were present when we did not use the DI water wash. These bubbles might be caused by the IPA over-primed surface, as discussed in Levinson [32], p. 57-59. The over-primed surface gets quickly contaminated by air pollutants. Thus, the DI water cleaning had to follow the IPA cleaning. The AMIW cleaned samples with the hard-bake procedure are shown in figure 1(e,g). There is no bubble formation on cleaned samples; however, the under-etching of the PMMA resist still occurs on the order of 2μm. The advantage of the negative resist is the possibility of further enhancing the resist adhesion to the surface by the increased electron beam dose. The datasheet recommended dose is 30 μC/cm^2. Instead, we used 200 μC/cm^2 and 10 nm step size and line spacing during the EBL exposure. The enhanced resist crosslinking is challenging later in resist stripping. However, since the underlying gold layer sustains a long time of oxygen etching, the resist can be stripped by the reactive ion etching (RIE) in oxygen (20 sccm, 5 min, 40 mTorr, 50 W).

3.2. Wet etching

We tested the over-exposed and hard-baked novolak resist in fabricating wet-etched gold ribbons on epitaxial graphene. The gold ribbons are nominally 500 nm wide, and the ribbon array has a periodicity of 3 μm. Besides the better resist adhesion compared to the PMMA, there is also an advantage of the negative resist in the possibility of the *in situ* visual inspection of the wet etching [29]. The exposed negative resist area is smaller than in the case of PMMA. Therefore the wet-etched gold area is much larger, allowing visual inspection of the etching process. The visual inspection is beneficial because the precise etching time is one of the critical parameters of successful wet etching. We compare three DAR-etched samples in figure 2. The three etching procedures differ by the etching time in DAR and by the order of the etched samples. The etching time is 10 s,

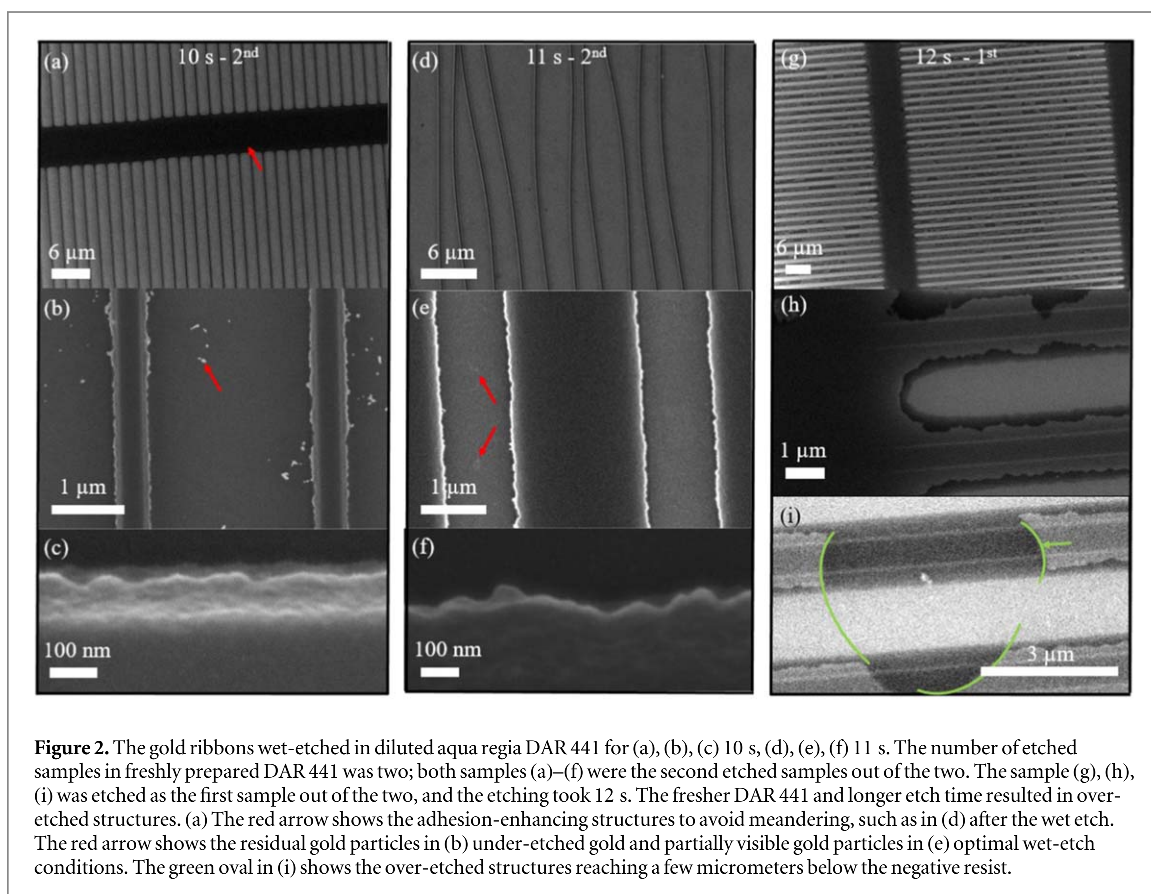

Figure 2. The gold ribbons wet-etched in diluted aqua regia DAR 441 for (a), (b), (c) 10 s, (d), (e), (f) 11 s. The number of etched samples in freshly prepared DAR 441 was two; both samples (a)–(f) were the second etched samples out of the two. The sample (g), (h), (i) was etched as the first sample out of the two, and the etching took 12 s. The fresher DAR 441 and longer etch time resulted in over-etched structures. (a) The red arrow shows the adhesion-enhancing structures to avoid meandering, such as in (d) after the wet etch. The red arrow shows the residual gold particles in (b) under-etched gold and partially visible gold particles in (e) optimal wet-etch conditions. The green oval in (i) shows the over-etched structures reaching a few micrometers below the negative resist.

11 s, and 12 s, as labeled in each column of figure 2. We always etched two samples using the same freshly prepared batch of DAR. Samples No. 1 and 2 were etched as the second sample; Sample No. 3 was etched as the first sample in the fresh DAR. The Sample No. 1, etched for 10 s, figures 2(a), (b), (c), shows minor traces of unetched gold, shown by the red arrow in figure 2(b). Sample No. 2 was etched for 11 s, and the unetched gold traces nearly vanished; see the two red arrows in figure 2(e). Sample No. 3 was etched as the first in the fresh-prepared DAR batch, and the etching time was 12 s. Both parameters (the first etched sample out of the two experiences stronger DAR, and 12s being the longest etch time) lead to over-etched gold with locally large etched holes, shown by the green curve in figure 2(i). The slight variation of etching time (10-12 s) and the etching order indicate that despite good resist adhesion to gold, the wet etching still requires precise adjustment of the etch parameters.

Further improvement to widen the etching time window could be achieved by diluting the aqua regia to weaker concentrations. We note that all etching was started within 1 min after preparing the fresh DAR batch. The DAR solution degrades on the order of minutes; hence, the etching properties will differ using the aged DAR.

When the gold ribbons were below 1-2 μm, we observed locally distorted ribbon arrays after wet etching, as depicted in figure 2(d). This effect is caused by shifted gold ribbon with the exposed resist during the post-etching dip in the DI water and drying. To avoid such distortion, we used mechanical stabilizers in the form of >2 μm wide stripes, shown by the red arrow in figure 2(a). We also dried the samples using nitrogen flow along the gold ribbons to minimize the forces exerted on the thin gold ribbons.

Finally, we stress the importance of a clean gold surface without any resist residua before the DAR etching. The resist residua will partially protect the gold from etching. However, DAR etches the resist slowly. After several seconds, the residual resist is penetrated by DAR, and rapid wet etching of gold commences. The residual resist thus makes the calibrated etching times exceedingly unreliable. Therefore, to make the etching time well-defined, the residual resist after the resist development has to be removed. We use 30 s RIE in oxygen plasma to remove the residual resist after the resist development.

The complete wet etching procedure is summarized in table 1, including AMIW cleaning, gold evaporation, spin coating, electron beam lithography, development, residual resist removal, hard bake, and wet etching. Particular attention must be paid to the clean sample's surface to avoid bubble formation after the hardbake. The overexposure of the negative resist with 10 nm step size and line spacing is also critical, as well as the residual resist removal, to achieve consistent etching time. Hardbake and well-optimized wet etching time are also

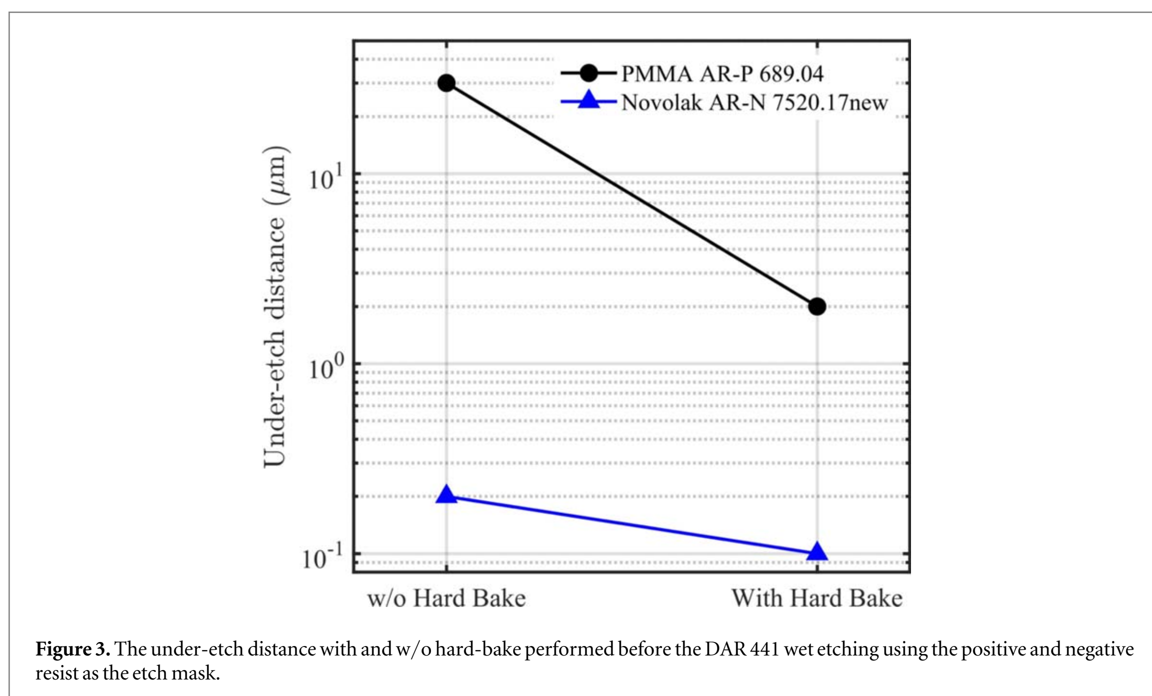

Figure 3. The under-etch distance with and w/o hard-bake performed before the DAR 441 wet etching using the positive and negative resist as the etch mask.

Table 1. The processing steps for wet etching of gold evaporated on the low-adhesion graphene surface.

Step no.	Process	Note
	AMIW cleaning	
1	acetone 5 min + methanol 5 min + IPA 5 min + DI water 10 min	Wafer cleaning to avoid bubbles after hard-bake
2	hot plate, 250 °C/900 s	Residual water removal
	E-beam evaporation	
3	30 nm Au, 2Å/s, 2.4×10^{-6} mbar	Au deposition
	Spin-coating	
4	negative resist AR-N 7520.17, 4000 rpm, 65 s	
5	hot plate 85 °C, 180 s	
	E-beam lithography	
6	$I = 1.3$ nA, step size 10 nm, line spacing 10 nm, dose 200 μC/cm^2	The high dose 200 μC/cm^2 is necessary to enhance adhesion of the resist to the wafer.
	Development	
7	AR 300-47, 6 min + DI water 30 s	resist development
8	RIE, O_2 20 sccm, 30 s, 40 mTorr, 50 W, 258 V_{DC}	residual resist removal
	Hard-bake	
9	hot plate, 85 °C, 180 s	Enhanced resistance against wet etching
	Wet etching	
10	DAR 441, 10 s + DI water 30 s	Diluted Aqua Regia, 4 parts (20 ml) of DI water, 4 parts (20 ml) of 37% HCl, 1 part (5 ml) of 69% HNO_3
11	Gentle drying by nitrogen 5-10 s. Blow the gas stream along thin structures.	Avoids mechanical distortion of small structures

critical. Despite the complex procedure, the wet etching of gold on graphene is feasible with minimized resist under-etching and adhesion problems.

The figure 3 compares the best lateral resolution achieved by the DAR wet etching of gold using the PMMA and negative resist as etching masks. The disadvantage of the PMMA is that it does not allow for enhancing the resist adhesion to the substrate by overexposing it during the electron beam lithography. The reason is that the PMMA is a positive-tone resist, resulting in reduced molecular size of PMMA molecules after the resist exposure, instead of enhanced resist adhesion to the gold surface, as in the case of the novolak negative resist.

3.3. Wet etching on uneven surfaces

Although the above-described wet etching works well on flat surfaces, there is still apparent under-etching when the negative resist is spin-coated on uneven or rough surfaces, as shown in figure 4 by red arrows. The reason is that the resist in the lower part of the edges is not fully attached to the substrate, forming small gaps. Such gaps

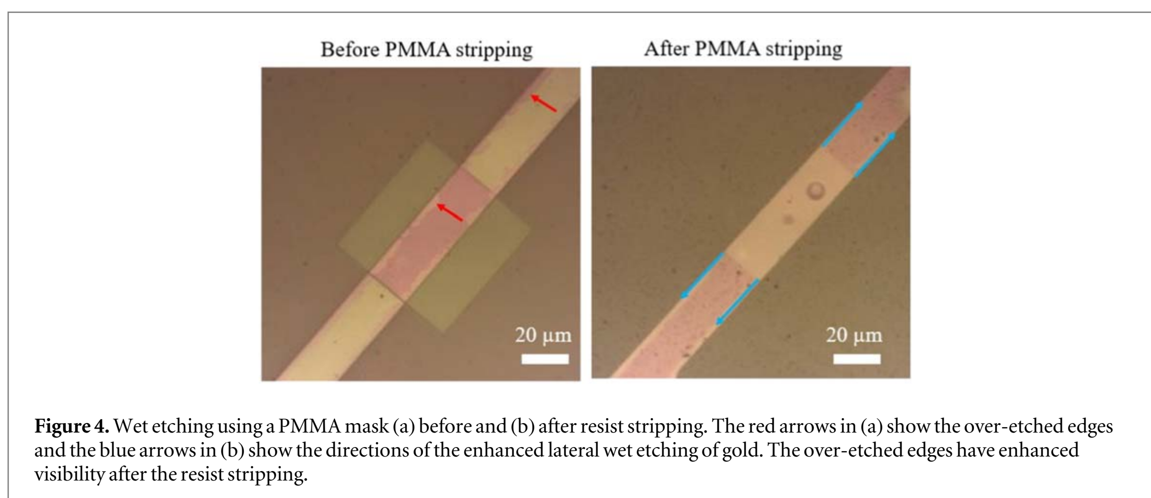

Figure 4. Wet etching using a PMMA mask (a) before and (b) after resist stripping. The red arrows in (a) show the over-etched edges and the blue arrows in (b) show the directions of the enhanced lateral wet etching of gold. The over-etched edges have enhanced visibility after the resist stripping.

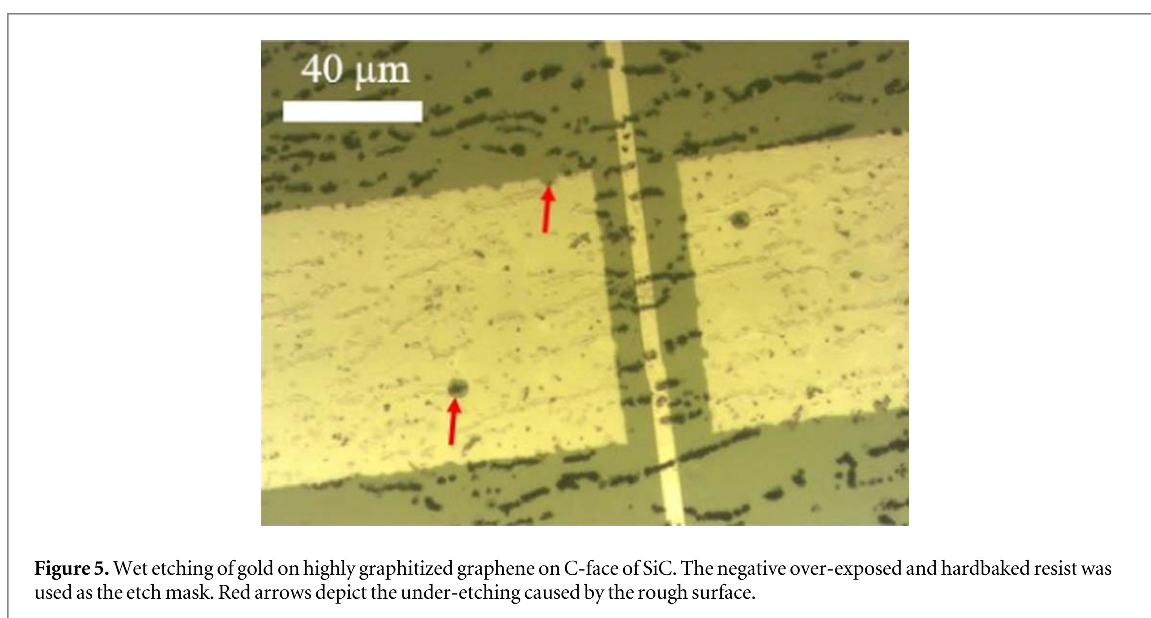

Figure 5. Wet etching of gold on highly graphitized graphene on C-face of SiC. The negative over-exposed and hardbaked resist was used as the etch mask. Red arrows depict the under-etching caused by the rough surface.

between the resist and the substrate cause strong capillary forces enforcing the flow of DAR along the edges. Blue arrows depict the direction of capillary forces along the step edges in figure 4. Therefore, the wet etching is much faster along step edges than the etching speed in the direction perpendicular to the sample's surface.

We demonstrate the case of the rough surface with DAR etched gold using the negative resist mask in figure 5. We use a highly graphitized C-face of SiC, which forms, besides the multi-layer epitaxial graphene, a large amount of deeply graphitized spots, as shown by black dots, and connected dots in figure 5. The rough surface leads to uneven resist thickness and etched holes within the mask, lower red arrow in figure 5. Similarly, the increased roughness leads to roughly etched edges, the top red arrow in figure 5. For these reasons, the gold wet etching should be performed on a smooth surface, and the etching must be one of the first nano-fabrication processes unless the lateral resolution can be compromised.

3.4. Aged gold

We also found that a sufficient delay between the gold evaporation and spin-coating leads to improved resist adhesion. Figure 6 shows wet etching of gold using PMMA and the novolak-based negative resists as the etch masks. We did not over-expose the negative resist or use the hardbake after the resist development. However, the delay between the gold evaporation and spin-coating was one year. It is known that the gold tarnishes due to atmospheric impurities (such as sulfur) or due to the impurities in the source material used for electron beam evaporation. The tarnished gold is sufficiently adhesive to the spin-coated resist without the need for further pre-processing. Since the year-long period is impractical, the aging can be partially replaced by extending the pre-processing procedure described in table 1. We propose to insert an additional resist ashing step in the pre-processing behind step No. 5., and to repeat the spin-coating steps No. 4 and 5, table 1. The ashed resist leaves

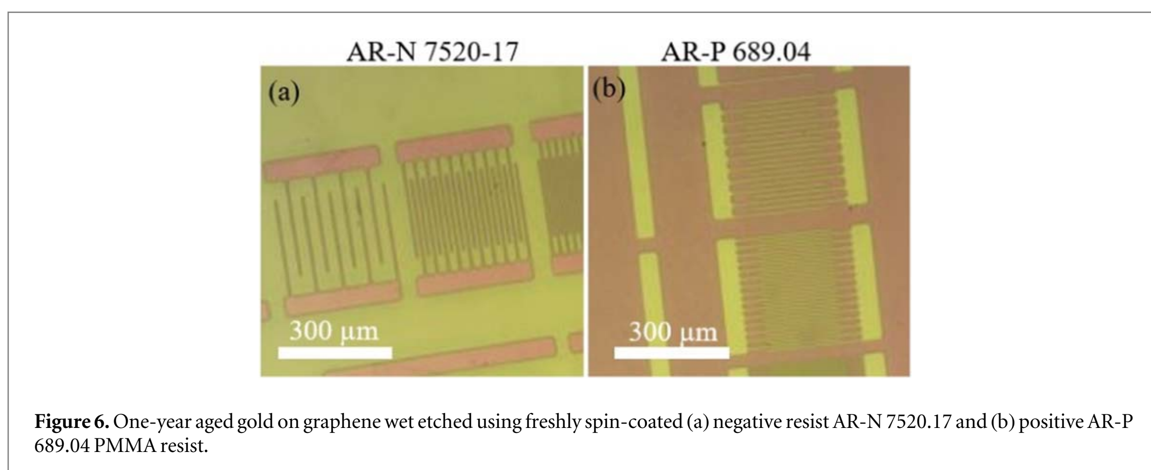

Figure 6. One-year aged gold on graphene wet etched using freshly spin-coated (a) negative resist AR-N 7520.17 and (b) positive AR-P 689.04 PMMA resist.

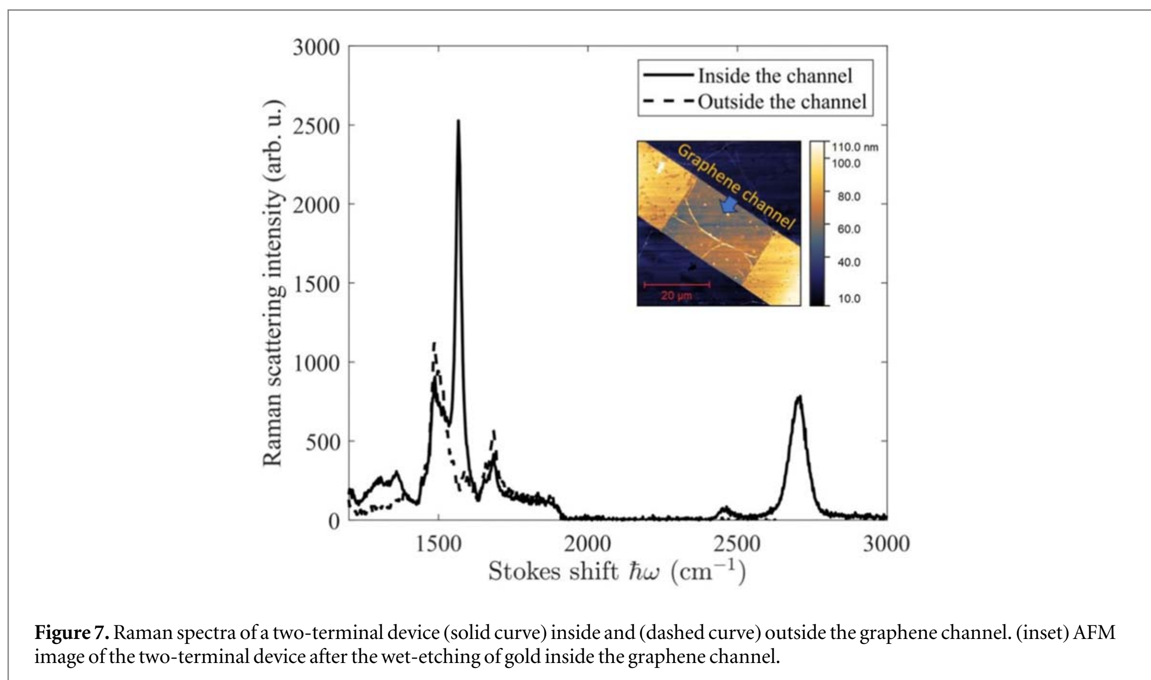

Figure 7. Raman spectra of a two-terminal device (solid curve) inside and (dashed curve) outside the graphene channel. (inset) AFM image of the two-terminal device after the wet-etching of gold inside the graphene channel.

traces of the residual resist on the gold surface, and the oxygen plasma used for the ashing leaves the surface activated. The following second spin-coating leads to improved resist adhesion to the gold surface.

3.5. Device characterization

We tested the capability of wet etching on a two-terminal device, see inset in figure 7 for the topography measured by Atomic Force Microscopy (AFM). The gold and graphene around the conducting path were dry-etched by the Reactive Ion Etching (RIE) (50 sccm Ar, 5 sccm O_2, 20 mTorr, 200 W, 75 s). The SiC mesa-structure was etched in SF_6-Ar mixture by RIE (10 sccm SF_6, 5 sccm Ar, 20 mTorr, 200 W, 20 s). We defined the graphene channel in the second lithographic step using the wet etching procedure described in table 1. The Raman spectra in figure 7 show the successful removal of graphene outside the channel and well-protected graphene inside the graphene channel. The electrical two-port resistance measurement led to 1–100 $k\Omega/sq$. The large variation of the square resistance reflects the device-to-device graphene inhomogeneity and lowered doping (increased resistance) caused by the wet etching. A similar charge-depletion of graphene after wet etching was observed previously [20].

4. Discussion

The DAR wet etching of gold can be further improved using a more diluted solution of aqua regia. The more diluted DAR will widen the time window for the optimal wet etching of gold. We demonstrated the optimal wet etching in the range of 10–12 s, which requires precise timing. The precise and reproducible timing is essential

for wet etching using the PMMA resist because the etching cannot be verified *in situ* visually during the etching. A similar effect, such as more dilute aqua regia, can be achieved by a more aged DAR. As the DAR ages, the volatile products nitrosyl chloride and chlorine gas evaporate, and the remaining water dilutes the DAR even further. Hence, the longer time after the DAR preparation will be equivalent to the more dilute DAR.

The wet etching of submicrometer structures is also prone to mechanical movement of small structures during the DI water cleaning after wet etching and drying in the nitrogen flow. The nitrogen flow effect can be reduced using the critical point dryer.

The hard-bake temperature could also be optimized to enhance the etching resistance to DAR. However, the temperature should not surpass the glass transition temperature T_{glass} of the resist. The glass transition temperature for the novolak AR-N 7520.17 is $T_{glass} \approx 102$ °C. When the hardbake temperature approaches or exceeds T_{glass}, the resist loses contact with the substrate at high temperature, and the adhesion does not recover after cooling the sample back below T_{glass}. Therefore, the hardbake at the temperature above T_{glass} can worsen the resist adhesion to the substrate.

The graphene device's cleanliness can be further improved by prolongated oxygen etching of the residual negative resist before wet etching. One can notice a small resist contamination in the inset of figure 7. This contamination comes from the negative resist deposited on gold in the first lithography step and defines the two-terminal device's conducting path.

Our nano-fabrication method can also be easily adapted to other materials, such as HgTe/HgCdTe heterostructures [34], ZnO/Ge core–shell nanowires [35] or silicon devices [30, 36], where the wet etching is an essential processing step. Notably, the electron beam exposure can be helpful when post-processing allows intense oxygen ashing of the remaining negative resist.

5. Conclusions

We demonstrated a procedure for wet etching of gold on graphene with 100's nm lateral resolution. We showed that the positive resist PMMA is only suitable for low-resolution etching. The key steps for successful wet etching are the following: to use a negative novolak-based resist, over-exposing the negative resist during the electron beam lithography, ashing the residual resist after development to achieve well-defined and repeatable etching times, hardbake at the temperature below the glass transition temperature, precise timing of DAR etching, and directional, small flow drying in the nitrogen stream. We demonstrated the effect of the lateral etching on the samples with an uneven and rough surface. We also showed the effect of surface contamination on the bubble formation after the hardbake. We also demonstrated the cleaning procedure of graphene grown epitaxially on SiC to avoid bubble formation. We also described that the resist adhesion could be further enhanced by gold aging or inserting one more ashing/spin-coating step in the pre-processing of DAR etching.

Acknowledgments

We acknowledge the joint international project of the Czech Science Foundation (GA ČR) and the National Research Foundation of Korea, project No. 21-28470J and NRF-2020K2A9A1A06103641, for financial support. CzechNanoLab project LM2023051 funded by MEYS CR is gratefully acknowledged for the financial support of the measurements and sample fabrication at CEITEC Nano Research Infrastructure.

Data availability statement

All data that support the findings of this study are included within the article (and any supplementary files).

Conflict of interest

The authors have no conflicts of interest to disclose.

CRediT authorship contribution statement

J Kunc: Methodology, conceptualization, data curation, fabrication, investigation, writing the original draft, review, and editing, funding acquisition. M Shestopalov: investigation, sample growth. J Jo: investigation, fabrication, draft editing. K Park: funding acquisition, investigation, draft editing.

Data access statement

The data supporting the findings of this study are available from the corresponding author upon reasonable request.

ORCID iDs

J Kunc https://orcid.org/0000-0001-8197-0890

J Jo https://orcid.org/0009-0007-9272-221X

K Park https://orcid.org/0000-0003-4086-7365

References

[1] Pirkle A *et al* 2011 *Appl. Phys. Lett.* **99** 122108
[2] Choi W, Shehzad M A, Park S and Seo Y 2017 *RSC Adv.* **7** 6943
[3] Goossens A M, Calado V E, Barreiro A, Watanabe K, Taniguchi T and Vandersypen L M K 2012 *Appl. Phys. Lett.* **100** 073110
[4] Lin Y-C, Lu C-C, Yeh C-H, Jin C, Suenaga K and Chiu P-W 2012 *Nano Lett.* **12** 414
[5] Kumar K, Kim Y-S and Yang E-H 2013 *Carbon* **65** 35
[6] Lin Y-C, Jin C, Lee J-C, Jen S-F, Suenaga K and Chiu P-W 2011 *ACS Nano* **5** 2362
[7] Paingad V C, Kunc J, Rejhon M, Rychetsky I, Mohelsky I, Orlita M and Kuzel P 2021 *Adv. Funct. Mater.* **31** 2105763
[8] Chaves F A, Jimenez D, Cummings A W and Roche S 2014 *J. Appl. Phys.* **115** 164513
[9] Jeon Y, Jung S, Jin H, Mo K, Kim K R, Park W-K, Han S-T and Park K 2017 *Sci. Rep.* **7** 16830
[10] Chaves F A, Jimenez D, Santos J E, Boggild P and Caridad J M 2019 *Nanoscale* **11** 10273
[11] Cheng Z, Zhou Q, Wang C, Li Q, Wang C and Fang Y 2011 *Nano Lett.* **11** 767
[12] Pham P V 2018 *Royal Society Open Science* **5** 172395
[13] Zhuang B, Li S, Li S and Yin J 2021 *Carbon* **173** 609
[14] Tyagi A *et al* 2022 *Nanoscale* **14** 2167
[15] Moser J, Barreiro A and Bachtold A 2007 *Appl. Phys. Lett.* **91**
[16] Choi W, Seo Y-S, Park J-Y, Kim K B, Jung J, Lee N, Seo Y and Hong S 2015 *IEEE Trans. Nanotechnol.* **14** 70
[17] Ma D, Zhang Y, Liu M, Ji Q, Gao T, Zhang Y and Liu Z 2013 *Nano Res.* **6** 671
[18] Sun J *et al* 2014 JACS **136** 6574
[19] Norimatsu W and Kusunoki M 2009 *Physica E-Low-Dimensional Systems & Nanostructures* **42** 691
[20] Yang Y, Huang L-I, Fukuyama Y, Liu F-H, Real M A, Barbara P, Liang C-T, Newell D B and Elmquist R E 2015 *Small* **11** 90
[21] Tzalenchuk A, Lara-Avila S, Kalaboukhov A, Paolillo S, Syvajarvi M, Yakimova R, Kazakova O, Janssen T J B M, Fal'ko V and Kubatkin S 2010 *Nat. Nanotechnol.* **5** 186
[22] Kruskopf M *et al* 2021 *IEEE Trans. Electron Devices* **68** 3672
[23] Janssen T J B M, Tzalenchuk A, Yakimova R, Kubatkin S, Lara-Avila S, Kopylov S and Fal'ko V I 2011 *Phys. Rev.* B **83**
[24] Williams K, Gupta K and Wasilik M 2003 *J. Microelectromech. Syst.* **12** 761
[25] Snow E H, Grove A S, Deal B E and Sah C T 1965 *J. Appl. Phys.* **36** 1664
[26] Stagg J P 1977 *Appl. Phys. Lett.* **31** 532
[27] Gabette L, Segaud R, Fadloun S, Avale X and Besson P 2009 Cleaning and surface conditioning technology in semiconductor device manufacturing 11 *ECS Transactions* ed T Hattori *et al* (Electrochem Soc; Elect & Photon Div) vol 25, pp 337–44 XI Int Symposium on Semicond Cleaning and Surface Conditioning Technol in Semicond Device Mfg held during the CCXVI Meeting of the Electrochemical-Soc (ECS), Vienna, AUSTRIA, OCT 04-09, 2009
[28] Ferguson M, Najah M, Banville F, Boucherit M, Miriyala N, Renaud J, Frechette L, Boone F, Ecoffey S and Charlebois S A 2022 *J. Electrochem. Soc.* **169** 083504
[29] Green T A 2014 *Gold Bull.* **47** 205
[30] Yoo J, Oh G, Kim M-W, Song S-H, Yoo S-D, Shim T-H and Kim E K 2019 *Nanotechnology* **30** 035205
[31] Mack C 2012 *Fundamental Principles of Optical Lithography, The Science of Microfabrication* (John Wiley Sons Ltd.) Reprint with correction May
[32] Levinson H J 2019 *Principles of Lithography* (Bellingham, Washington USA: SPIE Press) 4th edn (https://doi.org/10.1117/3.2525393)
[33] Kunc J, Rejhon M, Belas E, Dedic V, Moravec P and Franc J 2017 *Physical Review Applied* **8** 044011
[34] Shekhar P, Bendias K, Fuerst L, Liang X, Gbordzoe M K, Borzenko T, Buhmann H, Kleinlein J and Molenkamp L W 2023 *Nanotechnology* **34** 205302
[35] Sun Y-L, Zheng X-D, Jevasuwan W and Fukata N 2022 *Nanotechnology* **33** 325602
[36] Yamada K, Yamada M, Maki H and Itoh K M 2018 *Nanotechnology* **29** 28LT01